ROBUST CONTROLLERDESIGN WITHROAD ADAPTATION OF SEMI-ACTIVE SUSPENSION SYSTEM

THIẾT KẾ BỘ ĐIỀU KHIỂN BỀN VỮNG THÍCH ỨNG VỚI MẶT ĐƯỜNG CHO HỆ THỐNG TREO BÁN TÍCH CỰC

Vu Van Tan

ABSTRACT

Road profile is considered as an essential input that affects the vehicle dynamics, it is known for unknown input signal, depending on the velocity of the vehicle and the road class' roughness. Accurate information of this data is fundamental for a better understanding of the vehicle behaviour and vehicle control system design. In this present paper, the road profiles are generated according to the ISO 8606:2016 standard to compare the differential of the road profile when changing the conditions. The semi-active suspension techniques are the solution to this problem and capable of reducing road vibrations effectively. The vertical quarter car model is installed with semi-active suspension system using Electrorheological shock absorber (ER damper) also considered to study the response of the vehicle to the road profile. The H_∞ control method is used to design the controller for the semi-active suspension system by minimizing the closed-loop impact of disturbance and perturbation from the inputs to the controlled outputs. The comparison between the passive suspension and the semi-active suspension systemsare shown the positive effect of the robust controller scheme when enhancing two criteria of the vehicle oscillation are comfort and road holding.

Keywords: *Vehicle dynamics and control, Semi-active suspension system, Road adaptation,* H_∞ *control, Ridecomfort, Roadholding.*

TÓM TẮT

Mặt đường được coi là nguồn kích thích chủ yếu ảnh hưởng đến động lực học dao động của ô tô và được biết đến là tín hiệu đầu vào không xác định, tùy thuộc vào vận tốc chuyển động của ô tô cũng như độ mấp mô theo tường loại đường. Dữ liệu chính xác của biên dạng mặt đường là nền tảng cơ bản để hiểu rõ hơn về trạng thái của ô tô và thiết kế hệ thống điều khiển. Trong bài báo này, các biên dạng đường được thiết lập theo tiêu chuẩn ISO 8606:2016 để so sánh sự khác biệt khi thay đổi các điều kiện chuyển động. Các công nghệ của hệ thống treo bán tích cực là giải pháp cho vấn đề này và có khả năng dập tắt dao động của ô tô khi di chuyển trên đường một cách hiệu quả. Mô hình 1/4 ô tô được lắp đặt hệ thống treo bán tích cực sử dụng giảm chấn điện từ (ER) được xem xét để nghiên cứu đáp ứng của ô tô với các biên dạng mặt đường. Phương pháp được sử dụng để thiết kế bộ điều khiển cho hệ thống treo bán tích cực bằng cách giảm thiểu tác động vòng kín của nhiễu đầu vào tới các tín hiệu đầu ra được điều khiển. So sánh giữa hệ thống treo bị động và hệ thống treo bán tích cực cho thấy hiệu quả của cấu trúc điều khiển bền vững khi nâng cao cả hai tiêu chí cơ bản của hệ thống treo là độ êm dịu và độ bám đường.

Từ khóa: *Động lực học và điều khiển ô tô, hệ thống treo bán tích cực, thích ứng mặt đường, điều khiển bền vững, độ êm dịu chuyển động, độ an toàn chuyển động.*

Faculty of Mechanical Engineering, University of Transport and Communications
Email: vvtan@utc.edu.vn
Received: 01/11/2020
Revised: 15/12/2020
Accepted: 26/02/2021

1. INTRODUCTION

With the increase of demands for the ride comfort and roadholding performances, the intelligent suspension system has attracted high interest in recent decades, due to its commendable improvement inthis two criteria. Many systems are involved in cars to guarantee both safety (e.g. ABS, ESP, etc.) in [1] and comfort (e.g. suspensions, seats, etc.). The design of automotive control strategies for active force generators is an increasingly difficult task due to the growth in system complexity, reliability costs and time constraints. The vehicle active or semi-active suspension systems had been systematically investigated since the 1970s [2]. In recent decades, the studies of vehicle suspension systems have been focused on the control strategies and integrated control with other systems.

Concerning vehicle ride comfort and roadholding in normal cruise situation, it is well admitted that controlled suspension systems can provide good passenger isolation from road unevenness while keeping admissible the road holding performance. Industrial and academic research is very active in the automotive field; suspension design and control are important aspects for comfort and safety achievements. The controllers are designed and validated assuming that the actuator of the suspension is fully active. Unfortunately, these active actuators are not yet used on a wide range of vehicles because of their cost (e.g. energy, weight, volume, price, etc.) and low performance (e.g. time response); hence, in the industry, semi-active actuators (e.g. controlled dampers) are often preferred [3, 4].

The synergy between wheels and road surface causes a dynamic excitation which generates waves propagating in the soil, and impinging on the foundations of nearby structures [5]. At a particular, the dynamic properties of the suspension system, the vehicle speed and the elevation of the road surface unevenness determine the vehicle's vibration levels, consequently, the unpleasant of the passenger on the vehicle.

2. VEHICLE MODELLING

2.1. Artificial road profile creation

When the vehicle moving on the road with difference speed, the road disturbance in the spacedomain $Z_r(s)$ is a stationary process, but in the timedomain $Z_r(t)$is a non-stationary process. According to the mimic filter white

noise method based on the stable stochastic theory in [6, 7], the differential equation of road roughness in the spacedomain can be implemented as follows:

$$\dot{Z}_r(s) + \Omega_c Z_r(s) = 2\pi n_o \sqrt{S_q(n_o)} W(s) \quad (1)$$

Where Ω_c is the road spatial cut-off angular frequency, $\Omega = 2\pi n_c$;

n_c is the road spatial cut-off frequency, $n_c = 0.01(m^{-1})$;

n_0 is the standard spatial frequency, $n_0 = 0.1(m^{-1})$;

W(s) is the white noise in the spacedomain.

According to the space-time relationship, it has:

$$\dot{s}\frac{d}{ds} = \frac{d}{dt} \quad (2)$$

Substituting equation (2) into equation (1), the road excitation in the non-stationary running process can rewrite as:

$$\dot{Z}_r(t) + \dot{s}\Omega_c Z_r(t) = 2\pi n_c \dot{s}\sqrt{G_d(n_o)} W(t) \quad (3)$$

Where $\dot{s}$ is given as $\dot{s} = v_o + at$, in which, v_o is the initial vehicle velocity and ais the acceleration of the vehicle; t is the time running period of the vehicle and $G_d(n_o)$ is the road roughness coefficient.

We consider $a_1 = 2\pi n_c$, $b_1 = 2\pi n_o \sqrt{G_d(n_o)}$ so the equation (3) will become into:

$$\dot{Z}_r(t) + V.a_1.Z_r(t) = b_1.V.W(t) \quad (4)$$

According to the ISO 8608:2016 standard [8], the road is divided into several types from A to H, for each kind of road class, they provide the degree of road roughness. From equation (4) the values of $a_1$and $b_1$are calculated for each road type respectively as Table1.

Table 1. The value of a_1 and b_1 for each type of road profile

Class road	$G_d(n_0)10^{-6}$ [m^3]	a_1	b_1
A	16	0.062	$2.513x10^{-3}$
B	64	0.062	$5.026x10^{-3}$
C	256	0.062	0.010
D	1024	0.062	0.020
E	4094	0.062	0.040
F	16384	0.062	0.080
G	65536	0.062	0.161
H	262144	0.062	0.322

2.2. Quarter car modelling

A quarter car model represents a single corner of a vehicle with two degrees of freedoms (DOFs) is shown in Figure 1. This model contains the vertical chassis and wheel bounce displacement, allows studying only the vertical dynamic behaviour of the vehicle.

This simple model consists of the sprung mass m_s represents a quarter of the vehicle body (chassis). The unsprung mass m_{us} represents the wheel and the tire of the vehicle. z_s, z_{us} stand for the vertical displacement of the sprung mass m_s and the unsprung mass m_{us}, respectively. The suspension is composed by a spring with the stiffness coefficient k_s and a semi-active damper with the passive damper coefficient c_p when the semi-active damper is off. The tire is modelled by a spring with the stiffness coefficient k_t. Finally, z_r represents the road profile vertical disturbance.In this paper, the author uses a real car model installed in Gipsa-lab at the University Grenoble in France. It is named Soben car as shown in Figure 2. The parameters of the model are shown in Table2.

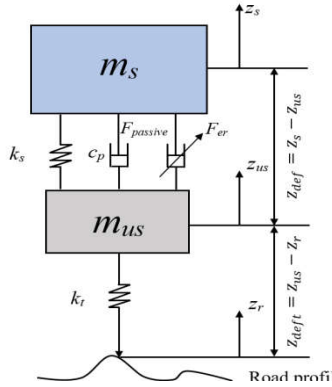

Figure 1. Quarter car model with semi-active suspension system

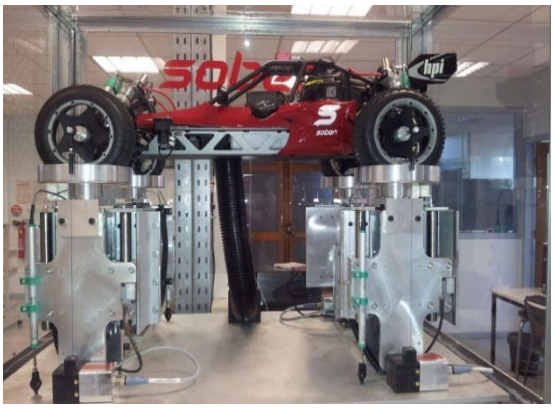

Figure 2. INOVE Soben car testbed in Gipsa-lab, France

Table 2. Parameter values of the quartercar model of Soben-car equipped with an ER damper

Parameters	Description	Value	Unit
m_s	Sprung mass	2.27	kg
m_{us}	Unsprung mass	0.25	kg
k_s	Spring stiffness	1396	N/m
k_t	Tire stiffness	12270	N/m
k_o	Passive damper stiffness coefficient	170.4	N/m
c_o	Viscous damping coefficient	68.83	Ns/m

From the second law of Newton for motion, the dynamical equations of the system around the equilibrium are given as:

$$\begin{cases} m_s\ddot{z}_s = -F_s - F_d \\ m_{us}\ddot{z}_{us} = F_s + F_d - F_t \end{cases} \quad (5)$$

Where F_s is suspension spring force, F_t is the tire force and the damper force F_d. $z_{def} = z_s - z_{us}$ and $\dot{z}_{def} = \dot{z}_s - \dot{z}_{us}$ are defined in turn as the suspension deflection and the suspension velocity. For the controloriented linear model, all of the suspension spring force and the tire force are considered as linear functions that are given by:

$$F_s = k_s(z_s - z_{us}) \quad (6)$$

$$F_t = k_t(z_{us} - z_r) \quad (7)$$

The damper force F_d is given as in (5) with deflection $x_d = z_{def} = z_u - z_{us}$. F_{erd} represents the desired force, which is generated by the semi-active damper to meet the requirements of control designing. Substituting (6), (7) into (5), one easily obtains:

$$\begin{cases} m_s\ddot{z}_s = -k_s(z_s - z_{us}) - k_o(z_s - z_{us}) - c_o(\dot{z}_s - \dot{z}_{us}) - F_{erd} \\ m_{us}\ddot{z}_{us} = k_s(z_s - z_{us}) + k_o(z_s - z_{us}) + c_o(\dot{z}_s - \dot{z}_{us}) + F_{erd} \\ \qquad -k_t(z_{us} - z_r) \end{cases} \quad (8)$$

From the equation (8) and the equation (4), the synthesis dynamic equations of the extended quarter car model are expressed as below:

$$\begin{cases} m_s\ddot{z}_s = k_s(z_s - z_{us}) - k_o(z_s - z_{us}) - c_o(\dot{z}_s - \dot{z}_{us}) - F_{erd} \\ m_{us}\ddot{z}_{us} = k_s(z_s - z_{us}) + k_o(z_s - z_{us}) + c_o(\dot{z}_s - \dot{z}_{us}) + F_{erd} \\ \qquad -k_t(z_{us} - z_r) \\ \qquad \dot{Z}_r(t) = -a_1.V.Z_r(t) + b_1.V.W(t) \end{cases} \quad (9)$$

3. DESIGNING THE H_∞ CONTROLLER

3.1. H_∞ control Problem

The H_∞ robust control theory for the physical system has been remarkable growth in its usage. Both industrial and academic communities have been interested in the use of the analysis and the synthesis tools that this control theory provides. Indeed, the H_∞ methods are used in control theory to synthesize controllers achieving stabilization with the guaranteed performance [9, 10].

The H_∞ control structure is given (see Figure 3), in which, $\sum(s)$ has two input vectors, the exogenous input wthat includes reference signal and disturbances, the manipulated variables u. There are two output vectors, the controlled output z that we would like to minimize and the measured variables y that are considered as the inputs of the controller K(s) to calculate the control signal u.

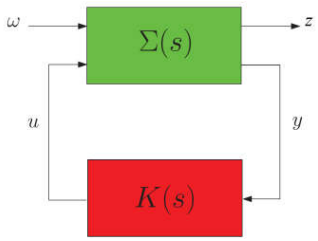

Figure 3. H_∞control problem scheme

The system in Figure 3 can be described as mathematically as follows:

$$\begin{bmatrix} \dot{x} \\ z \\ y \end{bmatrix} = \begin{bmatrix} A & B_1 & B_2 \\ C_1 & D_{11} & D_{12} \\ C_2 & D_{21} & D_{22} \end{bmatrix} \begin{bmatrix} x \\ w \\ u \end{bmatrix} \quad (10)$$

Where $x \in R^n$, $z \in R^r$, $y \in R^p$, $w \in R^q$, $u \in R^m$

H_∞ control problem is to find a controller which based on the information in measured outputs y, generates a control signal u which counteracts the influence of disturbance wto the controlled outputs z, thereby minimizing the closed-loop impact of disturbance and perturbation from the inputs and controlled outputs [10, 11].

The H_∞ controller K(s) is defined as follows:

$$\begin{bmatrix} \dot{x}_c \\ u \end{bmatrix} = \begin{bmatrix} A_c & B_c \\ C_c & D_c \end{bmatrix} \begin{bmatrix} x_c \\ y \end{bmatrix} \quad (11)$$

where $x_c \in R^n$, $y_c \in R^p$ and $u \in R^m$ are the state, the input and output of the controller, respectively.

The objective of the synthesis is to find a H_∞ controller K(s) of the form (11) such that the closed-loop system is quadratically stable and that, for a given positive real γ_∞, the L_2 induced norm of the operator mapping w to z is bounded by γ_∞:

$$\sup_{w \neq 0, w \in L_2} \frac{\|z\|_2}{\|w\|_2} \leq \gamma_\infty \quad (12)$$

3.2. H_∞ control design and solution

In the H_∞ framework, to satisfy the performance specifications, some weighting function $W_i(s)$ and $W_o(s)$ are added to the input disturbances and the controlled outputs as shown in the Figure 4. These weighting functions allow the shaping of some specific controlled output in the frequency domain. The interconnection between the weighting functions and the system $\sum(s)$ provides the generalized system P(s). The main idea of the H_∞ synthesis is to minimize the impact of the input disturbance $\tilde{w}$ on the controlled output $\tilde{z}$. The solution to the H_∞ control problem using dynamic output feedback for the system is given in the following:

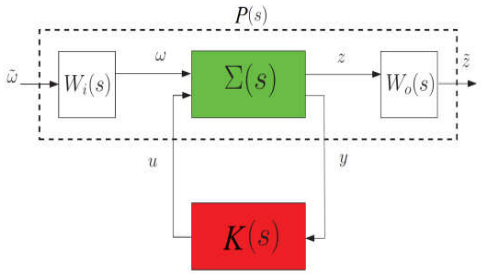

Figure 4. Generalized the H_∞control scheme

Consider the system, a dynamical output feedback controller K that solves the H_∞ control problem is obtained by the following LMIs in $(X, Y, \tilde{A}, \tilde{B}, \tilde{C}, \text{ and } \tilde{D})$ while minimizing γ_∞:

$$\begin{bmatrix} M_{11} & (*)^T & (*)^T & (*)^T \\ M_{21} & M_{22} & (*)^T & (*)^T \\ M_{31} & M_{32} & M_{33} & (*)^T \\ M_{41} & M_{42} & M_{43} & M_{44} \end{bmatrix} \prec 0 \quad (13)$$

$$\begin{bmatrix} X & I_n \\ I_n & Y \end{bmatrix} \succ 0$$

Where,

$$\begin{aligned} M_{11} &= AX + XA^T + B_2\tilde{C} + \tilde{C}^T B_2^T & M_{33} &= -\gamma_\infty I_m \\ M_{21} &= \tilde{A} + A^T + C_2^T \tilde{D}^T B_2^T & M_{41} &= C_1 X + D_{12}\tilde{C} \\ M_{22} &= YA + A^T Y + \tilde{B}C_2 + C_2^T \tilde{B}^T & M_{42} &= C_1 + D_{12}\tilde{D}C_2 \\ M_{31} &= B_1^T + D_{21}^T \tilde{D}^T B_2^T & M_{43} &= D_{11} + D_{12}\tilde{D}D_{21} \\ M_{31} &= B_2^T Y + D_{21}^T \tilde{B}^T & M_{44} &= -\gamma_\infty I_p \end{aligned} \quad (14)$$

Then, the controller K is obtained by the following equivalent transformation:

$$\begin{cases} D_c = \tilde{D} \\ C_c = (\tilde{C} - D_c C_2 X)M^{-T} \\ B_c = N^{-1}(\tilde{B} - YB_2 D_c) \\ A_c = N^{-1}(\tilde{A} - YAX - YB_2 D_c C_2 X - NB_c C_2 X - YB_2 C_c M^T)M^{-T} \end{cases} \quad (15)$$

Where M and N are defined such that $MN^T = I_n - XY$ which can be solved through a singular value decomposition plus a Cholesky factorization [10].

3.3. Design the H_∞ controller for the semi-active suspension system

3.3.1. General idea

The H_∞ control method is proposed here for the design of a semi-active suspension system, in which different optimization criterion is applied to guarantee the performance specifications. Two main criteria are considered to optimize: comfort and road-holding characteristics.

Specifically, the following signals are considered for performance analysis and characterization of a suspension system [3, 12]:

- To evaluate the comfort, the vertical acceleration $\ddot{z}_s$ of the chassis (sprung mass) is analyzed.
- To evaluate the roadholding, vertical displacement of the wheel z_{us} is analyzed.

3.3.2. Design H_∞ controller for the semi-active suspension system

To catch up with the goals of the suspension system, the controller is designed to adapt to the system. This Figure 5 describes the control structure for H_∞ controllers of the semi-active suspension system on the quarter car model, where includes the feedback structure of the model G and the compensator K. In the diagram, the signal u is the control input; $y_1$and y_2 are measured outputs, d_2 and d_3 are measured noises. The e_1, e_2, e_3 present as performance outputs of the force-controlled, the unsprung mass displacement and sprung mass acceleration.

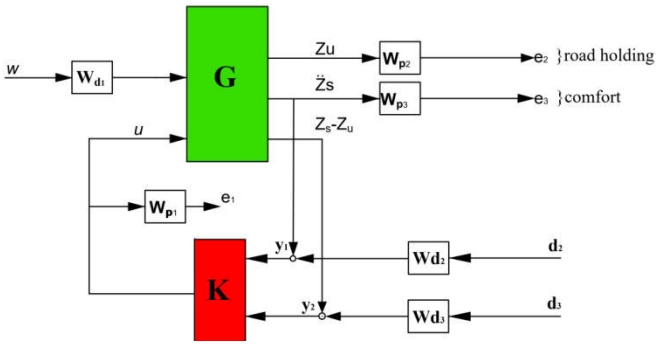

Figure 5. The diagram of the controller structure

The W_{d1} = 0.01 is used to shape the disturbance magnitudes, in this case, there are shaped to 1cm. W_{d2} and W_{d3} are selected as a diagonal matrix, which accounts for the sensor noise model in the control design that can enter the measurement signals. The noise weight of the unsung mass displacement sensor is chosen 10^{-4}(m); for the acceleration of the sprung mass is chosen 10^{-4}(m/s^2).

The weighting functions W_{p1}, W_{p2} and W_{p3} present the performance outputs signals, in [10, 12] the designer established the structure of them, also in [13], the writer illustrated a method by using Genetic Algorithms to select the optimal weighting function for the semi-active suspension system with H_∞/LPV synthesis. In this paper, the values of weighting functions are expressed as follows:

$W_{p1} = \dfrac{9}{s+14}$ weighting function for actuator;

$W_{p2} = 0.343\dfrac{s^2 + 35.14s + 618.51}{s^2 + 5.635s + 0.24}$ weighting function for theunsprung mass displacement;

$W_{p3} = 0.2\dfrac{2s^2 + 20.53s + 5.63}{2s^2 + 22.71s + 0.043}$ the weighting function of the sprung mass acceleration.

By selecting the system state vector as:

$x = \left[Z_s \quad \dot{Z}_s \quad Z_u \quad \dot{Z}_u \quad Z_r\right]^T,\ x \in R^5$

The measured output vector:

$y = \left[\ddot{Z}_s \quad Z_s - Z_u\right]^T, y \in R^2$

The control output vector:

$z = \left[Z_u \quad \ddot{Z}_s \quad Z_s - Z_u\right]^T, z \in R^3$

The disturbance and the control input vectors:

$w = W;\ u = F_{erd}$

The dynamical equations (9) of the quarter car model can be rewritten in the following state-space representation:

$$\begin{cases} \dot{x} = Ax + B_1 w + B_2 u \\ z = C_z + D_{1z} w + D_{2z} u \\ y = Cx + D_1 w + D_2 u \end{cases} \quad (16)$$

where the matrices $A, B_1, B_2, C, D_1, D_2, C_z, D_{1z}, D_{2z}$ are defined:

$$A = \begin{bmatrix} 0 & 1 & 0 & 0 & 0 \\ \frac{-k}{m_s} & \frac{-c_p}{m_s} & \frac{k}{m_s} & \frac{c_p}{m_s} & 0 \\ 0 & 0 & 0 & 1 & 0 \\ \frac{k}{m_u} & \frac{c_p}{m_u} & \frac{-(k+k_t)}{m_u} & \frac{-c_p}{m_u} & \frac{k_t}{m_u} \\ 0 & 0 & 0 & 0 & -a_1.V \end{bmatrix} \quad B_1 = \begin{bmatrix} 0 \\ 0 \\ 0 \\ 0 \\ b_1.V \end{bmatrix} \quad B_2 = \begin{bmatrix} 0 \\ \frac{-1}{m_s} \\ \frac{1}{m_u} \\ 0 \\ 0 \end{bmatrix}$$

$$C_z = \begin{bmatrix} 0 & 0 & 1 & 0 & 0 \\ \frac{-k}{m_s} & \frac{-c_p}{m_s} & \frac{k}{m_s} & \frac{c_p}{m_s} & 0 \\ 1 & 0 & -1 & 0 & 0 \end{bmatrix} \quad D_{1z} = \begin{bmatrix} 0 \\ 0 \\ 0 \end{bmatrix} \quad D_{2z} = \begin{bmatrix} 0 \\ \frac{-1}{m_s} \\ 0 \end{bmatrix}$$

$$C = \begin{bmatrix} \frac{-k}{m_s} & \frac{-c_p}{m_s} & \frac{k}{m_s} & \frac{c_p}{m_s} & 0 \\ 1 & 0 & -1 & 0 & 0 \end{bmatrix} \quad D_1 = \begin{bmatrix} 0 \\ 0 \end{bmatrix} \quad D_2 = \begin{bmatrix} \frac{-1}{m_s} \\ 0 \end{bmatrix}$$

4. SIMULATION RESULTS

4.1. Analysis of the results inthe frequency domain

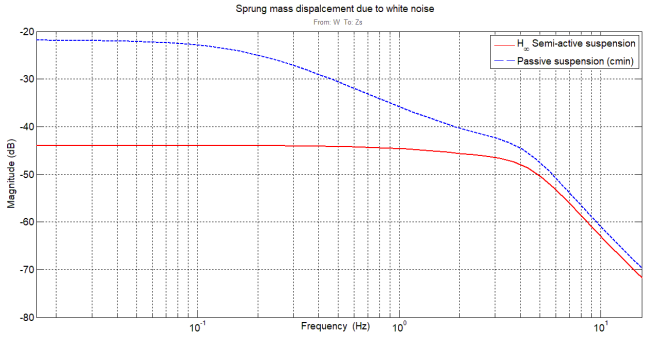

Figure 6. Frequency responds of the sprung mass displacement

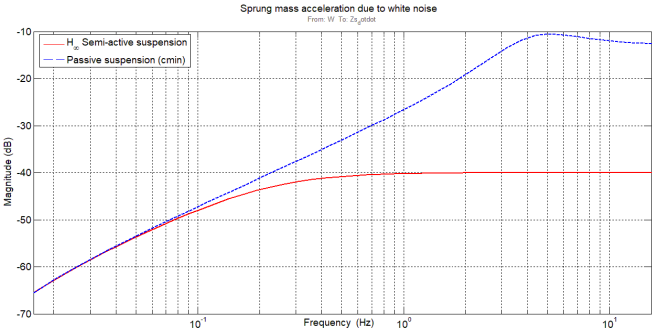

Figure 7. Frequency responds of the sprung mass acceleration

From Figures 6, 7, it can be seen that when using the H_∞ controller for the semi-active suspension system, the displacement of the sprung mass is reduced significantly. At low frequency (0 ÷ 5Hz), there is a decline from -40dB to -58dB when using the H_∞ controller for the system. Besides, the magnitude of the sprung mass acceleration not only reduces around 20dB in lower frequency but also remaining constants in the higher ones (10 ÷ 12Hz).

4.2. Analysis of the results in the time domain

From Figures 8, 9, it can be clearly seen that not only the displacement of the sprung mass is dropped but also the displacement of the unsprung mass as well. In the passive suspension system, the displacement of the sprung mass really high, for specific, from 0 to 0.8 second it raises substantially, in further time simulation, some moment it got over 7mm. However, the H_∞ controller guaranteed with the displacement of the sprung mass, by the way, the deflection of its magnitude around ±0.001m. The controlled force from the ER damper is shown in Figure 10. The comparison in two cases with the root mean square (RMS) value from the sprung mass and unsprung mass displacements is shown in Table 3. We can see that the effect of the robust controller in order to enhancing the comfort and road holding performances with the real Soben car.

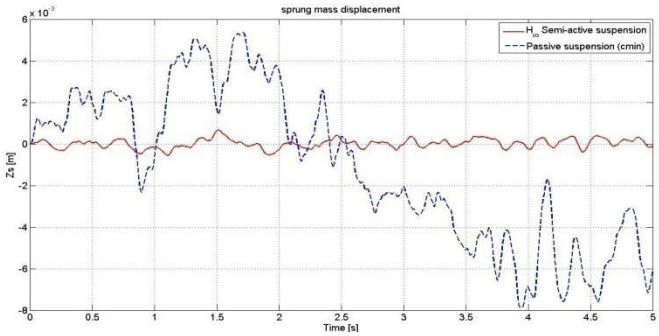

Figure 8. Time responds of the sprung mass displacement

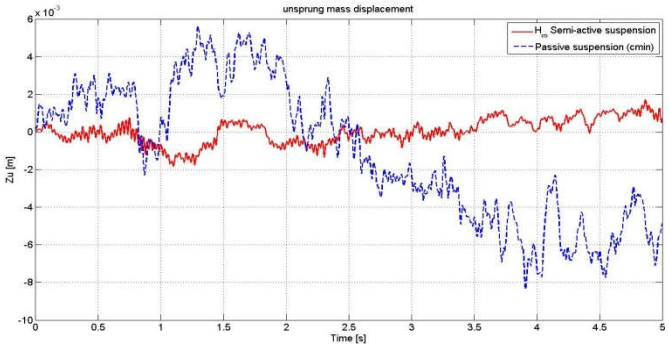

Figure 9. Time responds of the unsprung mass displacement

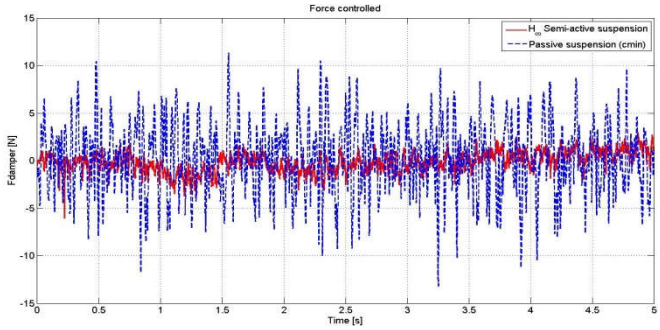

Figure 10. The controlled force of the ER damper in Soben car

Table 3. Compared the RMS of the sprung mass and unsprung mass displacements

	Z_u	Z_s
H_∞control	6.6843×10^{-4}	2.2204×10^{-4}
Passive	0.0036	0.0037
Reduction	81.43%	93.99%

5. CONCLUSIONS

In this paper, the background of the H_∞ control theory, the objective and the solutions of the control are illustrated, such that we can realize the advantages of the control strategy. The road profile is defined according to the ISO 8606:2016 as considering as a state of the system. The controller for the semi-active suspension system according to the H_∞ control theory is designed to improve the comfort and road holding characteristics. The results are presented above shows the effectof the controller in the frequency and time domains. The road holdingis improved up to 81% while the comfort about 94%.

In the future, we can validate the results with the real Soben car model based in Gipsa-lab. The vehicle will cross with different road classes while changing the speed, the development of the controller needs to adapt to the changing conditions of the vehicle.

ACKNOWLEDGEMENTS

The author would like to thank Professors Olivier Sename, Luc Dugard and their colleagues from University Grenoble Alpes, Francefor supporting the theory control knowledge and the experimental platform Soben car through the INOVE Project.

REFERENCES

[1]. CornoSavaresi, TanelliFabbri, 2009. *Control-oriented steering dynamics analysis in sport motorcycles: modelling, identification and experiments*. IFAC-papersonline, Volumes 42, Issue 10, 468-473.

[2]. Thomas D. Gillespie, 1992. *Fundamentals of vehicle dynamics*. SAE International publishing.

[3]. Sergio M. Savaresi, Charles Poussot-Vassal, Cristiano Spelta, Olivier Sename, Luc Dugard, 2010. *Semi-active suspension control design for vehicles*. Elsevier book.

[4]. C. Poussot-Vassal, O. Sename, L. Dugard, P. Gaspar, Z. Szabo, J. Bokor, 2008. *A new semi-active suspension control strategy through LPV technique*. Control Engineering Practice, Volume 16, 1519-1534.

[5]. Wei Liu, Ruochen Wang, Renkai Ding, Xiangpeng Meng, LinYang, 2020. *Online estimation of road profile in semi-active suspension based on unsprung mass acceleration*. Mechanical Systems and Signal Processing, Volume 135.

[6]. Feng Tyan, Yu-Fen Hong, Shun-Hsu Tu, Wes S. Jeg, 2009. *Generation of random road profiles*. Journal of Advanced Engineering, Volume 4, 1373-1378.

[7]. Kazem Reza-Kashyzadeh, Mohammad Jafar Ostad-Ahmad-Ghorabi, Alireza Arghavan, 2017. *Investigating the effect of road roughness on automotive component.* Engineering Failure Analysis, Volume 41, 96-107.

[8]. ISO 8606:2016 standard.

[9]. Harry L. Trentelman, Anton A. Stoorvogel, Malo Hautus, 2012. *Control theory of linear system*. Springer book.

[10]. Olivier Sename, 2016. *Robust and LPV control of MIMO systems. Part 2: H∞ control*. University Grenoble Alpes, France.

[11]. Olivier Sename, 2017. *Robust control of MIMO systems*. University Grenoble Alpes, France.

[12]. Carlos Vivas-Lopez, Diana Hernández Alcántara, Manh Quan Nguyen, Soheib Fergani, Gabriel Buche, Olivier Sename, Luc Dugard, Rubén Morales-Menéndez, 2014. *INOVE: a testbench for the analysis and control of automotive vertical dynamics*. 14th International Conference on Vehicle System Dynamics, Identification and Anomalies (VSDIA 2014), 403-413.

[13]. Anh Lam Do, Cristiano Spelta, Sergio Savaresi, Olivier Sename, Luc Dugard, Diego Delvecchio, 2010. *An LPV control approach for comfort and suspension travel improvements of semi-active suspension systems*. 49th IEEE Conference on Decision and Control (CDC), 5560-5565.

[14]. Thanh Phong Pham, Olivier Sename, Luc Dugard, 2019. *Design and Experimental Validation of an H_∞ Observer for Vehicle Damper Force Estimation*. 9th IFAC International Symposium on Advances in Automotive Control (ACC), Volume 52(5), 673-678.

THÔNG TIN TÁC GIẢ

Vũ Văn Tấn

Khoa Cơ khí, Trường Đại học Giao thông Vận tải